# BETHE-HEITLER MUON BACKGROUND AT A MUON COLLIDER*

S.A. Kahn[#], M.A. Cummings, T.J. Roberts, Muons, Inc., Batavia, IL, 60510, U.S.A.

D. Hedin, A. Morris, Northern Illinois University, DeKalb, IL 60115, U.S.A

J. Kozminski, Lewis University, Romeoville, IL, 60446, U.S.A.

## Abstract

Multi-TeV muon colliders are an important option for a future energy frontier lepton collider since synchrotron radiation in a circular collider is significantly less than that expected in an electron collider. Muon decays are a major source of beam induced backgrounds that can affect the physics seen in a muon collider. For a muon collider with 750 GeV $\mu^+\mu^-$ with $2\times10^{12}$ $\mu$ per bunch we would expect $8.6\times10^5$ muon decays per meter for the two beams. These backgrounds include electrons from muon decays, synchrotron radiation from the decay electrons, hadrons produced by photo-nuclear interactions, coherent and incoherent beam-beam pair production and Bethe-Heitler (B-H) muon production. This paper will describe a simulation of the B-H muon production in a muon collider. These muons can penetrate the collider ring magnets and shielding and can enter into the detector region. This simulation tracks B-H muons produced in the collider ring in the range of ±175 m from the interaction point.

## INTRODUCTION

Historically electron-positron colliders have been a powerful tool for the measurements of new phenomena in high energy physics. However as the energy of $e^+e^-$ colliders increases, the energy loss due to bremsstrahlung in circular colliders and beamstrahlung in linear colliders eventually limit the maximum energy achievable in these machines. Because the energy loss of a charged particle due to radiation is inversely proportional to $m^4$, a $\mu^+\mu^-$ collider should have the potential of achieving higher center of mass energy than an $e^+e^-$ collider. Since muons decay, a muon collider will have a large background due to the extremely energetic products of these decays. The size of the accelerator-based backgrounds is dependent on the number of muon decays per unit length. For a muon collider with 1.5 TeV center-of-mass energy with parameters listed in Table 1, we would expect $8.6\times10^5$ muon decays per meter for both muon beams. A study of beam induced backgrounds in a muon collider with a 10° conical shield in the forward/backward direction is also submitted to this conference [1] and previous conferences [2]. In this paper we concentrate on the Bethe-Heitler muon background. When energetic photons in the electro-magnetic shower from the muon decay electrons interact with matter in the magnets and shielding muon pairs can be produced similar to electron pair production. The muon pair production rate is smaller than the electron pair production by a factor of $(m_e/m_\mu)^2$. Although this rate is small, the muons can penetrate through the magnet and shielding material into the detector region.

Table 1:Parameters describing the 1.5 TeV com Muon Collider Ring

| Parameter | Value |
|---|---|
| Center-of-Mass Energy | 1.5 TeV |
| Energy of Each Beam | 750 GeV |
| Luminosity | $10^{34}$ cm$^{-2}$sec$^{-1}$ |
| Bunches per Fill | 1 |
| Muons/Bunch | $2\times10^{12}$ |
| Repetition Rate | 15 Hz |
| Ring Circumference | 2.6 Km |
| Shielding Angle | 10° |

## SIMULATION MODEL

For this study, muon decay electrons are simulated in the muon collider ring using the G4beamline program [3]. The magnetic optics used for the collider ring are described in the lattice conceptual design [4,5]. The magnets for the final focus and the chromatic correction regions are included in the model which extends to ±175 m from the intersection point (IP). Figure 1 shows the magnets of the lattice in the vicinity of the IP. As muons can penetrate deeply into magnet and shielding material, these materials must be included in the simulation. In our study the collider ring and detector hall are surrounded with 0.75 m of concrete, and the region outside of the concrete is surrounded by earth since the collider ring is likely to be 200 m below the ground. Since the muons penetrate the magnet coil and yoke, the field must be supplied both for the magnet aperture, the coil and for the iron return yoke where the field will be in the opposite direction. Muon decays are distributed uniformly along the muon reference orbit with the Michel energy distribution boosted to the lab frame. As the cross section rate for muon pair production is quite small it was necessary to increase this cross section (by a factor of $5\times10^4$) to obtain a sufficient number of events and to appropriately weight the events. As long as the B-H cross section is not increased so much that a single decay electron produces multiple muon pairs, this procedure should not bias the results.
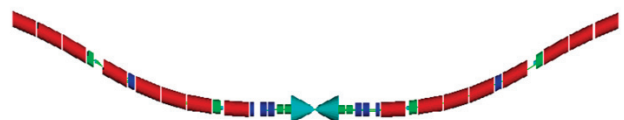


Figure 1: Sketch of the collider ring lattice in the vicinity of the IP. The figure shows the magnets ±75 m from the IP.

Bethe-Heitler muons are mostly a concern for the calorimeter where the presence of an energetic muon can affect the physics. For the detector in the study, we used tracking planes and calorimeter elements with dimensions, materials, and locations similar to those proposed for the SiD detector [6]. Particles are tracked to a minimum kinetic energy of 5 MeV due to the time required to generate and process the Monte Carlo events. Fortunately, it is the more energetic muons that are important for this study. Figure 2, which shows the muon hits as they enter the calorimeter, indicates that the muons hits are predominantly in the forward/backward calorimeters. These hits are recorded for our study. The muons are tracked in the calorimeter, but the energy deposited is not recorded. Figure 3 shows the muon hits as a function of the physics variables, $\phi$ (azimuth) and $\eta$ (pseudo-rapidity). The events at $|\eta| > 1.1$ are in the end calorimeters. There is an enhancement in hits at $\phi=0$ and $\pi$.
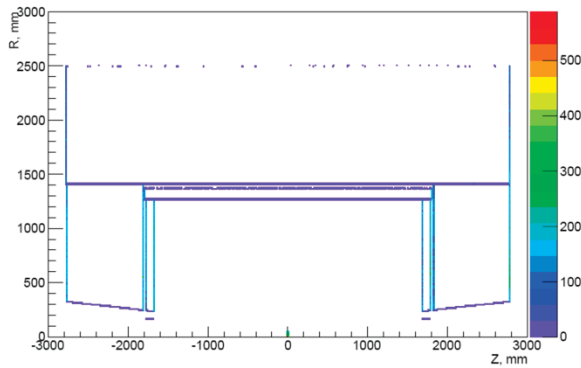


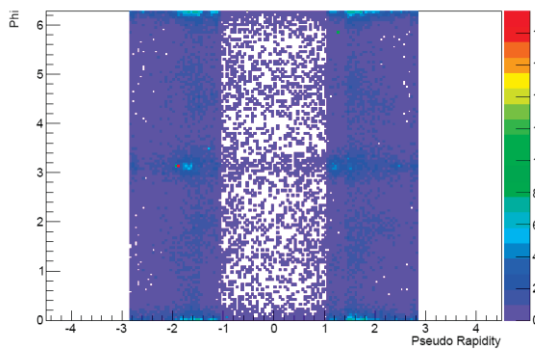Figure 2: R-Z plot of the muon hits entering the calorimeter regions.



Figure 3: Muon hits in the calorimeter as a function of the detector physics variables: $\phi$ and $\eta$.

## CHARACTERISTICS OF B-H MUONS

Since the muons can penetrate the surrounding material, muons can travel a significant distance before entering the detector. Figure 4 shows the Z-position of the primary muon decay that produces the muon that will finally reach the calorimeter. The muons from the positive beam coming from the left shown in red from the muons produced by the negative beam coming from the right shown in blue. The asymmetry between the negative and

positive beams is being investigated. Bethe-Heitler muons entering the calorimeter can come from muon decays as far as ±125 m from the IP.
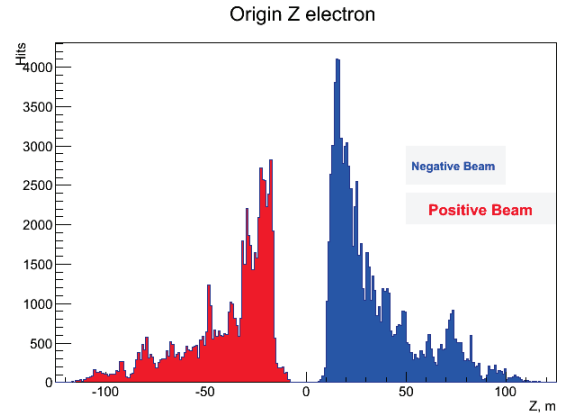


Figure 4: Origin of the muons that reach the detector calorimeter.

Figure 5 and 6 show the kinetic energy spectrum for B-H muons entering the backward (left), central (center) and forward (right) hadron calorimeters. The mean kinetic energy is ~3.5 GeV in the forward/backward calorimeters and ~2.5 GeV in the central calorimeter. The distribution extends to above 250 GeV.
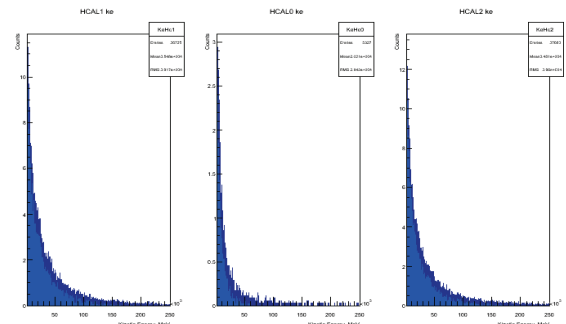


Figure 5: Kinetic Energy distribution of B-H muons entering the backward (left), central (center) and forward (right) hadron calorimeters. The KE is in GeV.
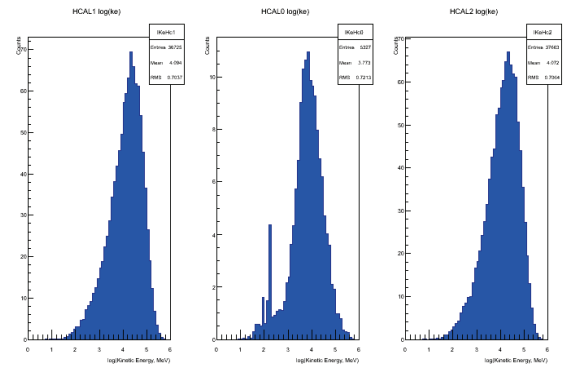


Figure 6: $\log_{10}$(KE) distribution for B-H muons entering the backward(left), central (center) and forward (right) hadron calorimeters. The KE is in MeV.

## MUON TIMING AND RATES

B-H muons will take a different path to the detector than particles from physics related processes. One can expect to reduce the contribution from B-H muons by imposing a time gate on the data acquisition. In Figure 7 we compare the arrival time of B-H muons into the hadron calorimeter to the expected arrival of a particle coming from an interaction in time with a beam-beam crossing and traveling at the speed of light from the IP. The figure separates B-H muons coming from $\mu^+$ (top row) and $\mu^-$ (bottom row) decays. B-H muons originating with $\mu^+$ ($\mu^-$) will be cleanly separated from IP related tracks in the backward (forward) calorimeter. Conversely B-H muons originating with $\mu^+$ ($\mu^-$) will overlap in time in the forward (backward) calorimeter with tracks arriving from the IP in time with the beam crossing. Most B-H muons in the central calorimeter will be out of time with tracks arriving from the IP in time with the beam crossing.
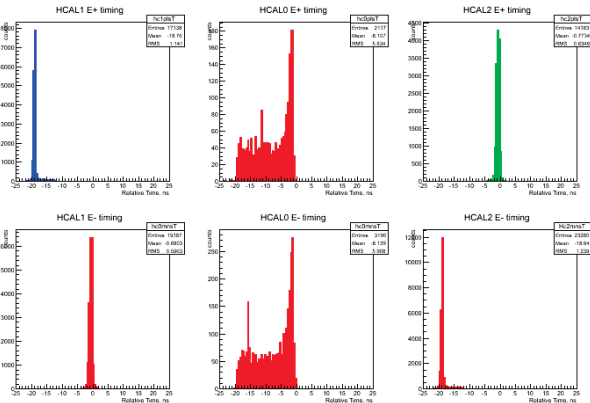


Figure 7: Difference in flight time of B-H muons when compared with a track arriving from the IP in time with the beam crossing. The top (bottom) row show time differences from $\mu^+$ ($\mu^-$) beams. The columns correspond to the backward, central and forward calorimeters.

Tables 2 and 3 show the number of B-H muon tracks expected in the hadron and electromagnetic calorimeters for a beam crossing with $2\times10^{12}$ muons per bunch in each of the beams. The tables also show the effect of imposing a 1 ns, 500 ps and 100 ps gate for the data acquisition. While 1 ns timing may be achievable, the 500 ps and 100 ps timing for calorimeters is beyond the current technology. Regardless, even a 1 ns timing cut is an effective tool in reducing the B-H muon background.

Table 2: B-H muon hits expected in the hadron calorimeter for $2\times10^{12}$ muons per bunch in each beam.

| Timing Cut | Backward Calorimeter | Central Calorimeter | Forward Calorimeter |
|---|---|---|---|
| No Cut | 1064 | 151 | 1069 |
| 1 ns | 399 | 4 | 267 |
| 500 ps | 212 | 0.6 | 141 |
| 100 ps | 45 | 0 | 27 |

Table 3: B-H muon hits expected in the electromagnetic calorimeter for $2\times10^{12}$ muons per bunch in each beam.

| Cut | Backward Calorimeter | Central Calorimeter | Forward Calorimeter |
|---|---|---|---|
| No Cut | 939 | 213 | 949 |
| 1 ns | 390 | 1 | 260 |
| 500 ps | 206 | 0 | 137 |
| 100 ps | 47 | 0 | 27 |

## REFERENCES

[1] M.A.C. Cummings et al., "Muon Collider Detector backgrounds", IPAC12, New Orleans, MOPPC036 (2012).

[2] S.A. Kahn et al., "Beam Induced Detector Backgrounds at a Muon Collider", PAC11, New York, (2011), p 2300.

[3] T. Roberts and D. Kaplan, "G4beamline Simulation Program for Matter Dominated Beamlines", Proc. of PAC07, p3468, http://g4beamline.muonsinc.com

[4] Y. Alexahin et al., "Conceptual Design of the Muon Collider Ring Lattice", Proc. of IPAC10, Kyoto, http://accelconf.web.cern.ch/AccelConf/IPAC10/papers/tupeb021.pdf

[5] Y. Alexahin et al., "Muon Collider Interaction Region Design", Proc. of IPAC10, Kyoto, http://accelconf.web.cern.ch/AccelConf/IPAC10/papers/tupeb022.pdf

[6] SiD Detector Outline Document, http://hep.uchicago.edu/~oreglia/siddod.pdf